

# Numerical Analysis of Thermal-Hydrological Conditions in the Single Heater Test at Yucca Mountain

*Jens T. Birkholzer and Yvonne W. Tsang*  
*Earth Sciences Division, Lawrence Berkeley National Laboratory*  
*Berkeley, CA, 94720*

## Introduction

The Single Heater Test (SHT) is one of two *in-situ* thermal tests included in the site characterization program for the potential underground nuclear waste repository at Yucca Mountain. The heating phase of the SHT started in August 1996, and was completed in May 1997 after 9 months of heating. The coupled processes in the unsaturated fractured rock mass around the heater were monitored by numerous sensors for thermal, hydrological, mechanical and chemical data. In addition to passive monitoring, active testing of the rock mass moisture content was performed using geophysical methods and air injection testing. The extensive data set available from this test gives a unique opportunity to improve our understanding of the thermal-hydrological situation in the natural setting of the repository rocks. The present paper focuses on the 3-D numerical simulation of the thermal-hydrological processes in the SHT using TOUGH2. In our comparative analysis, we are particularly interested in the accuracy of different fracture-matrix-interaction concepts such as the Effective Continuum (ECM), the Dual Continuum (DKM), and the Multiple Interacting Continua (MINC) method.

## Test Configuration

The SHT consists of a 5 m long, nominal 4 kW heating element, horizontally placed among 30 instrumented boreholes, which span a block of approximately 13 m x 10 m x 13 m in a side alcove of the underground Exploratory Studies facility (ESF) at Yucca Mountain. The test block resides in the potential repository formation of the Topopah Spring welded tuff approximately 200 m above the groundwater table. Though the welded tuff has very low matrix permeability, it is intensely fractured with the fracture permeability several orders of magnitude higher than the matrix permeability. At ambient conditions, the fractures are essentially drained and not very conductive to water. However, strong capillary forces hold a significant amount of water in the matrix pores. This water can be mobilized due to the heating of the rock mass, raising the liquid saturation in the fractures, so that the water flux in the fractures can be enhanced by several orders of magnitude from its ambient values.

### **3-D Numerical Model of the SHT**

Modeling of the thermal-hydrological processes in the SHT is carried out using the EOS4 module of the TOUGH2 simulator (Pruess, 1991). The fractured tuff in the test block is conceptualized using an Equivalent Continuum (ECM), a Dual Continuum (DKM), and a Multiple Interacting Continua (MINC) formulation, respectively. All these conceptual models appropriately describe the characteristics of unsaturated flow in fractures and matrix; however, they differ in the way fracture-matrix interaction is treated. The ECM is the most simplified method; it assumes that a local thermodynamic equilibrium is maintained between the fractures and the matrix at all times, thus implying infinitely fast mass and energy exchange between fractures and matrix. The DKM conceptualizes the fractured rock as two interacting continua, one representing the matrix, one representing the fractures, with the fracture-matrix exchange explicitly calculated from the local pressure and temperature difference. Thus the DKM can account for the different transient behavior of fractures and matrix. However, it sometimes tends to underestimate fracture-matrix interaction particularly for fast and rapid perturbations at early times, when steep gradients can occur at the fracture-matrix interfaces. Such steep gradients can not be appropriately modeled with the DKM because a linear pressure/temperature distribution is assumed within the matrix blocks. The MINC method solves this problem by subdividing the matrix continuum into a number of nested continua defined at different distances from the surface. This concept allows for representing a non-linear distribution of pressure or temperature in the matrix; therefore the MINC method should be best suited for simulating a localized and intense thermal perturbation such as that encountered in the SHT.

The hydrological and thermal input parameters used in the numerical simulations for the SHT are mainly determined from site-specific measurements, such as the matrix properties and fracture permeability values. Fracture characteristic parameters, which have not been directly measured, are extracted from mountain-scale calibrations performed for the ambient present-day flow field. Possible chemical or mechanical alterations in response to the heating are not included in our model. The initial conditions for the model domain were chosen as 87.0 kPa for gas pressure, 25 °C for temperature, and 0.92 for matrix saturation, as given by pre-heating characterization of the SHT. Details concerning the model input parameters and initial conditions are given in Birkholzer & Tsang (1996).

The computational domain for the thermal-hydrological simulations includes the entire 3D SHT block plus significant rock volumes added in all directions to guarantee a proper definition of boundary conditions. Small grid blocks are used around the heater hole to be compatible with sharp gradients of temperature, saturation and pressure. The 3D grid for the single continuum ECM simulations comprises about 30,000 grid blocks and more than 100,000 connections between them. Compared to that, the number of grid blocks used for the DKM and MINC runs increases by a factor of 2 and a factor of 5, respectively, indicating that the latter methods are extremely computationally intensive.

## Simulation Results

Introducing a heat source in the unsaturated fractured tuff at Yucca Mountain gives rise to strong two-phase flow effects, typically characterized as follows:

- (1) drying of the rock and vaporization of pore water close to the heater,
- (2) vapor transport away from the heated area due to gas pressure build-up,
- (3) condensation of the vapor in cooler regions outside of the drying zone,
- (4) reflux of condensate to the vicinity of the heating due to capillary suction, and
- (5) drainage of water away from the heated area due to gravity.

These processes are reflected in the spatial variation and temporal evolution of the liquid saturation in the rock mass. They also contribute to heat transfer in the near-field environment, as heat-induced gas and liquid fluxes may give rise to significant convective heat transport. For example, strong vapor-liquid counterflow may be reflected in a distinct "heat pipe" temperature signal, i.e., the temperature values remain at the nominal boiling point for some time before they continue to increase. Thus, close analysis of the numerous temperature measurements in the SHT can help to identify and constrain moisture redistribution characteristics, while the comparison of measured and modeled temperatures may serve to determine the suitability of different modeling conceptualizations in describing heat-induced flow and transport processes.

As a typical example for the temperatures observed in the SHT, we present the time evolution of measured temperature at one particular sensor located approximately 0.7 m away from the heater borehole in Figure 1. The down spikes register incidences of power outages. Temperature increases to nominal boiling within about 50 days, and continues to increase without evidencing a significant heat pipe signal. Since the other sensor observations show similar trends, the temperature data indicate that the SHT hydrogeological and thermal properties allow for only limited liquid reflux from the condensation zone back to the heater; i.e., heat conduction appears to account for most of the temperature rise. Figure 1 also gives the simulated results, obtained using the ECM, DKM, and MINC method, respectively. Note that the ECM results display only one temperature curve due to the local equilibrium assumption, while DKM and MINC have separate curves for fracture and matrix temperatures. In the latter case, the measured temperature values should be compared with the simulated matrix results, as the sensor is placed in a grouted borehole. Generally, the agreement between the measured and simulated data is very good for the three models, indicating that the thermal-hydrological response of the SHT is well represented. However, the ECM results display a subtle heat pipe signal, which retards the temperature increase at nominal boiling for some time and gives rise to a slight underestimation of temperature for the remaining heating period. The temperature curves obtained with the DKM and MINC method are almost identical: Both simulated matrix curves match the measured data curve exactly without showing a heat pipe signature. The fracture temperatures, on the other hand, display a distinct plateau at nominal boiling, indicative of substantial vapor-liquid counterflow.

Analysis of the simulated moisture redistribution processes demonstrates more substantial differences between the three model concepts ECM, DKM, and MINC. Figure 2 shows the matrix saturation at 3 months heating for a vertical plane in the mid-plane of the heater. (The heater borehole is located in the center perpendicular to the cross-section displayed.) In all three cases, drying occurs up to a radial distance of about 1 to 1.5 meters from the heater; beyond that is the condensation zone where liquid saturation is higher than at ambient conditions. While strong gravity drainage in the fractures is obtained using DKM, indicated by the saturation build-up below the heater, no gravity drainage is observed using the ECM. The ECM concept involves the crucial assumption that pressure equilibrium between the fractures and matrix is maintained at all times. As a result, gravity driven liquid flow in the fractures tends to be underestimated, since vapor condensing on the fracture walls is readily imbibed into the matrix pores and driven back towards the heater. The MINC approach yields moisture redistribution processes bounded by the two "extreme" model concepts DKM and the ECM. Geophysical data seem to indicate that the moisture content below the heater is larger than above, suggesting that gravity drainage is present during the heating phase. However, the data at this point do not allow to clearly state which one of the two models, DKM or MINC, is better suited in representing the thermal-hydrological processes.

## Summary

In the present paper, we have simulated the thermal-hydrological processes in the SHT using a 3D numerical model of the fractured tuff in the heater vicinity. Three different fracture-matrix conceptualizations were employed, the ECM, the DKM, and the MINC method. Generally we obtained a reasonably good agreement between data and simulation results for all three models. A closer analysis shows that the ECM method is least capable of capturing the transient nature of the processes in the SHT. In order to clearly discriminate between the DKM and MINC conceptual models, more data and more analysis is needed.

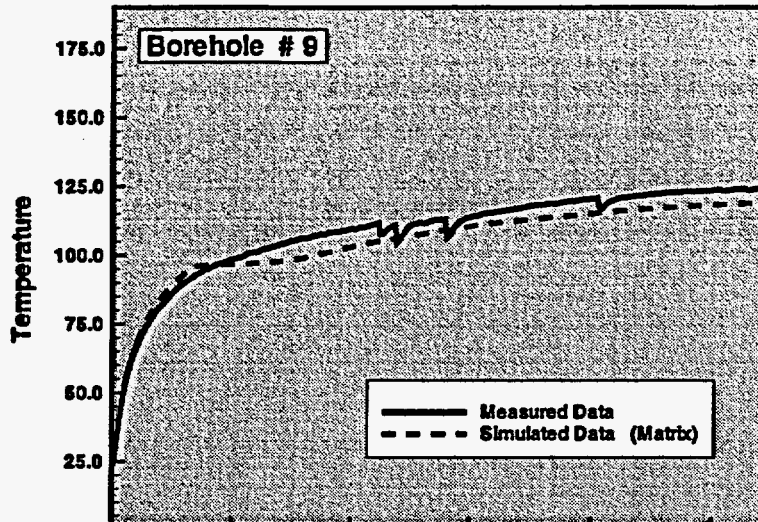
## References

- Birkholzer, J.T. and Y. W. Tsang, 1996. Forecast of thermal-hydrological conditions and air injection test results of the Single Heater Test at Yucca Mountain, LBNL-39789, E.O. Lawrence Berkeley National Laboratory, Berkeley, California.
- Pruess, K., 1991. TOUGH2 — A general purpose numerical simulator for multiphase fluid and heat flow, LBL-29400, UC-251, Lawrence Berkeley National Laboratory, Berkeley, CA.

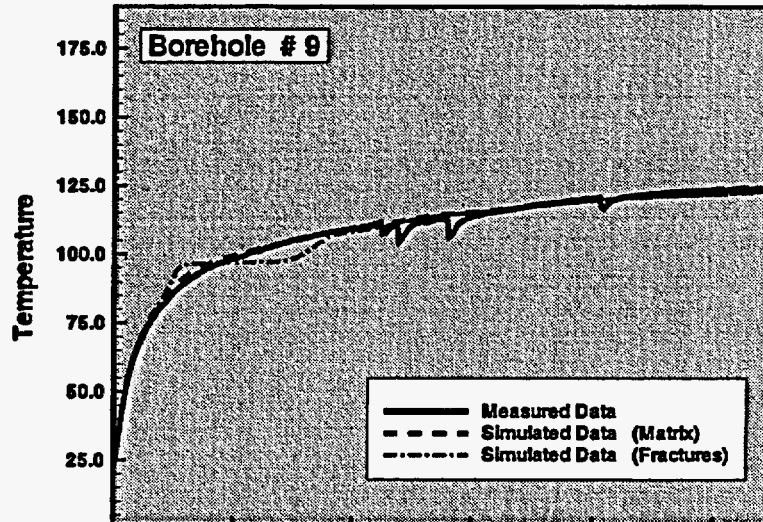
## Acknowledgment

We thank C. Oldenburg and R. Trautz for their review of the manuscript and comments for improvement. This work was supported by the Director, Office of Civilian Radioactive Waste Management, U.S. Department of Energy, through Memorandum Purchase Order EA9013MC5X between TRW Environmental Safety Systems, Inc. and the Ernest Orlando Lawrence Berkeley National Laboratory, under Contract No. DE-AC03-76SF00098.

ECM



DKM



MINC

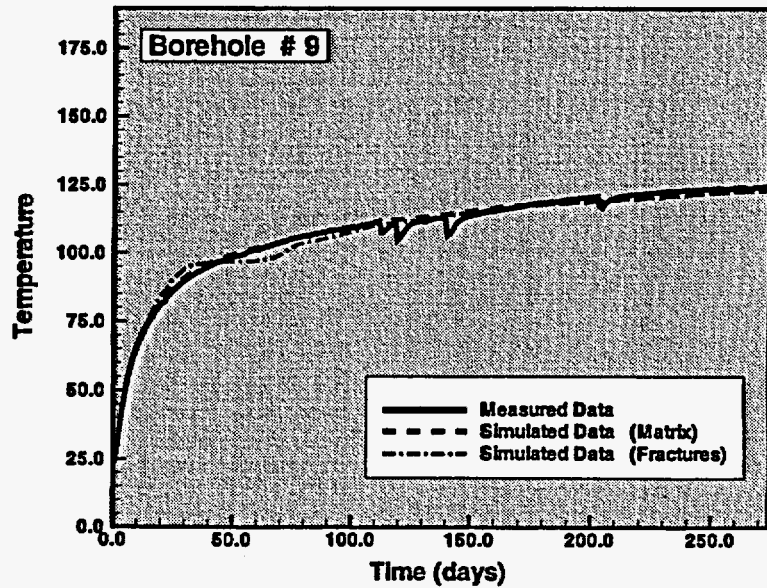
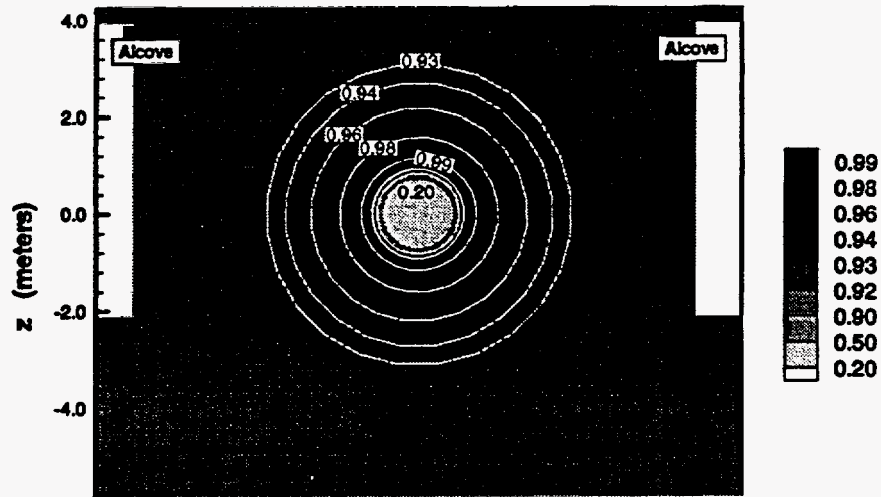


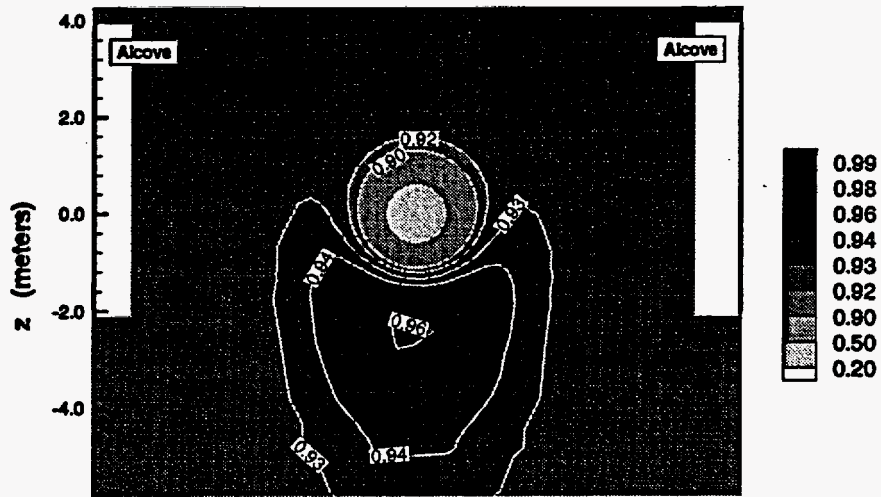
Figure 1: Measured versus simulated temperature evolution for ECM, DKM, and MINC



ECM



DKM



MINC

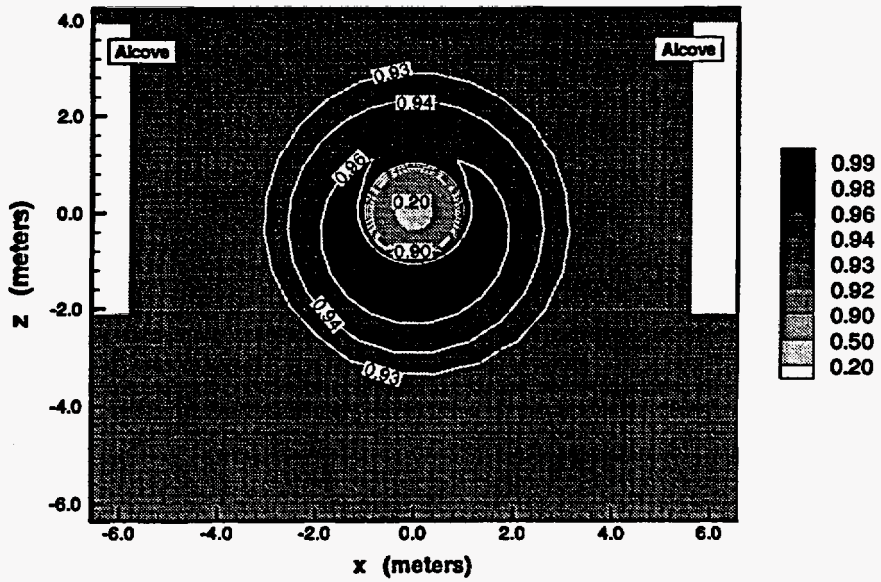


Figure 2: Simulated matrix saturation at 3 months of heating for ECM, DKM, and MINC